ISSN 1066-3622, Radiochemistry, 2012, Vol. 54, No. 4, pp. 395–400. © Pleiades Publishing, Inc., 2012.
Published in Russian in Radiokhimiya, 2012, Vol. 54, No. 4, pp. 364–368.

Synthesis, Labeling, and Biological Evaluation of 2-{[Benzyl(cyanomethyl)amino]methyl}-3-(ethoxycarbonyl)-quinoxaline 1,4-Dioxide in Ascites Bearing Mice[1]

I. T. Ibrahim*[a], M. A. Waly[b], and M. El-Tawoosy[a]

[a] *Labelled Compounds Department, Radioisotopes Production and Radioactive Sources Division, Hot Laboratories Center, Atomic Energy Authority, P.O. Box 13759, Cairo, Egypt;*
** e-mail: ismailtaha_73@yahoo.com*

[b] *Chemistry Department, Faculty of Science (Damiatta), Mansoura University, Mansoura, Egypt*

Received September 5, 2011

Abstract—Quinoxaline 1,4-dioxide derivative, 2-{[benzyl(cyanomethyl)amino]methyl}-3-(ethoxycarbonyl) quinoxaline 1,4-dioxide (Q_3D), was synthesized and labeled with radioiodine via direct electrophilic substitution giving labeling yield above 90%. The product was examined by paper electrophoresis. ^{125}I-Q_3D was prepared using Chloramine T as oxidizing agent. ^{125}I-Q_3D was stable for up to 72 h post labeling, in contrast to ^{99m}Tc-AQCD which is stable only for a short time. Biodistribution study of ^{125}I-Q_3D in ascites tumor bearing mice revealed large uptake of the labeled compound in tumor sites. In addition, in vitro incubation of the labeled compound with Ehrlich cells indicated incorporation of these compounds in DNA of tumor cells. This uptake of ^{125}I-Q_3D in DNA of tumor cells may be helpful in tumor diagnosis and therapy.

Keywords: quinoxaline, iodine, labeling, biodistribution, ascites, DNA

DOI: 10.1134/S1066362212040157

Quinoxaline (benzopyrazine) is a heterocyclic compound containing fused benzene and pyrazine rings. It is an isomer of quinazoline. The synthesis and chemistry of quinoxalines have attracted considerable attention in the last years [1]. Quinoxaline 1,4-di-*N*-oxide derivatives seem to have very interesting anticancer activity [2]. Also, some of them exhibit biological activity, in particular, antiviral, antibacterial, antiinflammatory, and antiprotozoal activity [2]. The antitumor activity of these compounds was observed mainly on solid tumors containing hypoxic cells, as quinoxalines act by bioreductive alkylation of DNA of cancer cells [3]. In addition, some of them exhibit activity against Ehrlich ascites carcinoma. Labeling of some of these derivatives was attempted to study the biodistribution of these compounds and also to know the possible mechanism of action [4]. Biodistribution study of ^{99m}Tc-3-amino-2-quinoxalinecarbonitrile 1,4-dioxide against ascites tumor showed concentration of the labeled compound in tumor sites [5]. ^{99m}Tc-labeled quinoxaline derivatives may be suitable for imaging purposes, despite their low stability. Iodine labeling may overcome this drawback, and also the Auger effect of iodine may contribute to the cytotoxic effect of quinoxaline, especially when it become near the DNA [6].

In this study, we synthesized 2-{[benzyl(cyanomethyl)amino]methyl}-3-(ethoxycarbonyl)quinoxaline 1,4-dioxide (Q_3D), performed its iodine labeling using Chloramine T as an oxidizing agent, and examined the factors affecting the labeling yield. Biodistribution of the labeled compound in normal and ascites bearing mice was also studied. In addition, ^{125}I-Q_3D was incubated with Ehrlich cells in vitro. DNA of Ehrlich cells was separated by centrifugation at high speed and counted for activity in a γ-ray counter.

EXPERIMENTAL

Drugs and chemicals. Iodine-125 was purchased from the Institute of Isotope Production, Belguim. Benzofurazan oxide, malononitrile, dimethyl formal (DMF), triethylamine, and diethyl ether were supplied from ICN (USA). Chloramine T was purchased from Sigma (USA). 3-Benzylaminopropionitrile was purchased from Alfa Aesar (CAS 706-03-6). All the other chemicals were of analytical grade (AR), obtained from reputed manufacturers. Ehrlich ascites carcinoma (EAC) was kindly supplied from the National Cancer Institute, Cairo, Egypt.

[1] The text was submitted by the authors in English.

Animals. Female Swiss Albino mice weighing 20–25 g were purchased from the Institute of Eye Research, Cairo, Egypt. The environmental and nutritional conditions were kept constant throughout the experimental period. The mice were kept at room temperature (22 ± 2°C) with a 12 h on/off light schedule. Female mice were used in this study because their susceptibility to Ehrlich ascites carcinoma was higher than that of the male mice [7]. Animals were kept with free access to food and water throughout the experiment.

Synthesis of Q_3D. The scheme of the synthesis of the target compound **3** is shown below. The quinoxaline derivative with active methyl group in the side chain **1** [8] was brominated with *N*-bromosuccinimide (NBS) in the presence of benzoyl peroxide as a catalyst in CCl_4 to obtain quinoxaline bromomethyl derivative **2** in 73.7% yield. The ^{1}H NMR spectrum of bromomethyl derivative **2** reflects the presence of CH_2Br protons at δ 4.75 ppm.

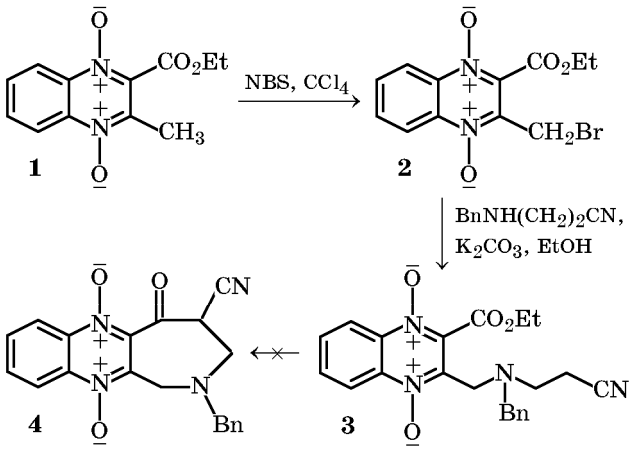

Quinoxaline bromomethyl derivative **2** was reacted with 3-(benzylamino)propionitrile in the presence of potassium carbonate in ethanol to obtain target compound **3**. Compound **3** is hygroscopic and should be kept under anhydrous conditions. The IR spectrum of **3** contains the cyano group absorption band at 2234 cm^{-1}. Its ^{1}H NMR spectrum shows the presence of five methylene protons at δ 2.23, 3.12, 4.11, 4.33, and 4.89 ppm. Attempted cyclization of **3** under widely varied conditions (bases, solvents, temperatures) failed to give the azepinoquinoxaline ring system, and the decomposition occurred instead.

2-(Bromomethyl)-3-(ethoxycarbonyl)quinoxaline 1,4-dioxide 2. *N*-Bromosuccinimide (1.95 g, 0.011 mol) was added to a solution of 2-(ethoxycarbonyl)-3-methylquinoxaline 1,4-dioxide **1** (2.48 g, 0.01 mol) in CCl_4 (50 ml) and $CHCl_3$ (50 ml) in the presence of benzoyl peroxide (0.20 g) as initiator. The solution was stirred and heated under reflux for 24 h. The organic layer was washed with cold water (3 × 30 ml), dried over anhydrous Na_2SO_4, and evaporated in a vacuum to give an oily material. The resulting oil was triturated with diethyl ether and recrystallized from 90% ethanol to give pure product **2** (2.41 g, 73.7% yield), mp 112–114°C. IR (KBr, ν, cm^{-1}): 1739 (CO), 1346 (N–O). ^{1}H NMR ($CDCl_3$), δ, ppm: 1.52 t (3H, *J* = 7.2 Hz, CH_3, ester), 4.63 q (2H, *J* = 7.2 Hz, CH_2, ester), 4.75 s (2H, CH_2Br), 7.84–7.90 m (4H, Qu). Calculated for $C_{12}H_{11}BrN_2O_4$ (*M* = 327.13): C 44.06; H 3.39; N 8.56. Found: C 44.36; H 3.65; N 8.30.

2-{[Benzyl(2-cyanoethyl)amino]methyl}-3-(ethoxycarbonyl)quinoxaline 1,4-dioxide. A solution of **2** (1.6 g, 0.005 mol) and 3-*N*-benzylaminopropionitrile in ethanol (30 ml), with potassium carbonate (3 g) added, was refluxed for 4 h. The mixture was poured into cold water (50 ml), and the precipitate was filtered off. Recrystallization from ethanol gave pure product **3** (1.1 g), mp 98°C. IR (KBr, ν, cm^{-1}): 2234 (CN) and 1710 (CO, ester). ^{1}H NMR ($CDCl_3$), δ, ppm: 1.43 t (3H, *J* = 7.2 Hz, CH_3, ester), 2.23 t (2H, *J* = 7.3 Hz, CH_2CH_2CN), 3.12 t (2H, *J* = 7.3 Hz, CH_2CH_2CN), 4.11 q (2H, *J* = 7.2 Hz, CH_2, ester), 4.33 s (2H, CH_2Ph), 4.89 s (2H, QuCH_2), 7.65–7.90 m (9H, aromatic). Calculated for $C_{22}H_{22}N_4O_4$ (*M* = 406.43): C 65.01; H 5.46; N 13.78. Found: C 65.34; H 5.75; N 13.40.

Iodine labeling. ^{125}I-Q_3D was prepared by the following procedure: 1 mg of Q_3D was dissolved in 1 ml of DMF with stirring. A 10 : 1 (w/w) solution of Chloramine T (CAT) in double-distilled water was prepared, and 50–100 μg was added to 100 μl of Q_3D solution in a dark colored tube, after which approximately 50–100 MBq of ^{125}I was added at room temperature. After a specified interval of time, the reaction was stopped by adding a 0.2 N $Na_2S_2O_3$ solution to reduce the unchanged iodine before chromatographic analysis [9]. The product yield and radiochemical purity were determined by paper electrophoresis. In the process, free iodide moved toward the anode at the top, whereas the target compound persisted near the point of spotting.

Factors affecting labeling yield. With the aim of optimizing the synthesis conditions, we examined the effect of the following factors on the labeling yield: oxidant amount (10, 25, 50, and 100 μg), Q_3D amount

(10, 25, 50, 100, and 200 μg), pH (2, 4, 7, 9, 11; measured with a Model 601 A-digital pH meter, Orion Research, USA), and reaction time (1, 5, 10, 30, and 60 min). When varying one of the parameters, the other parameters were kept constant.

In vitro stability. The target product content was determined at different time intervals (1, 4, 12, 24, and 48 h) after labeling.

Electrophoresis. Electrophoresis was done with an EC 3000 p-series 90 programmable power and chamber supply units using cellulose acetate strips (45 cm). These strips were moistened with 0.05 M phosphate buffer pH 7 and then introduced in the chamber. Samples were applied at a distance of 10 cm from the cathode. The strips were kept in the electric field for 1.5 h. The developed strips were dried and cut into 1-cm segments, which were counted with a well-type NaI scintillation counter. The radiochemical yield was calculated as the ratio of the radioactivity of the labeled product to the total radioactivity [9].

Tumor transplantation in mice. Ehrlich ascites carcinoma cells (EAC) are a model for studying the biological behavior of malignant tumors and drugs assumed to produce effect at these sites [10].

A line of Ehrlich ascites carcinoma (EAC) was maintained in female Swiss Albino mice through weekly I.P. transplantation of 2.5×10^6 tumor cells per mouse. EAC cells were obtained by needle aspiration under aseptic conditions. The ascitic fluid was diluted with sterile saline so that 0.1 ml contained 2.5×10^6 cells counted microscopically using a hemocytometer. About 0.2 ml of the solution was then injected intraperitoneally in the peritoneal cavity to produce acites tumor [11].

Biodistribution of ^{125}I-Q_3D in normal mice. In vivo biodistribution studies were performed using four groups of six mice each. Each animal was injected in the tail vein with 0.2 ml of the solution containing 5–10 kBq of ^{125}I-Q_3D. The mice were kept in metabolic cages for the required time. Animals were sacrificed by cervical dislocation at the recommended time (15 min, 1 h, 4 h, or 24 h) after injection. The organs or tissues of interest were removed, washed with saline, weighed, and counted. Correction was made for the background radiation and physical decay during the experiment. The weights of blood, bone, and muscles were assumed to be 7, 10 and 40% of the total body weight, respectively [9].

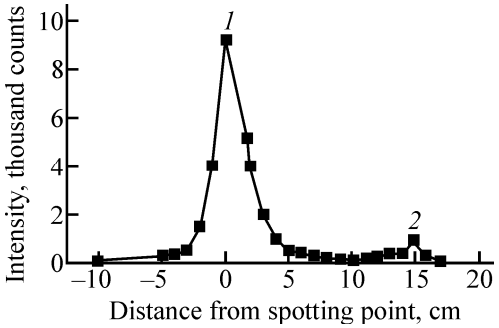

Paper electrophoresis pattern of radioiodinated Q_3D.

Biodistribution of ^{125}I-Q_3D in ascites tumor bearing mice. A group of 24 ascites tumor bearing mice was used for studying the biodistibution of the labeled drug. Experiments were performed in the same manner as with normal mice. Ascites fluid was drained and counted as a whole in a well type NaI(Tl) γ-ray counter. The results were calculated as percentage of injected dose (I.D.) per gram of tissue [12].

DNA extraction. Extraction of the DNA from the tumor helps to study the incorporation rate of radioactivity in the tumor. Ehrlich cells were drained from ascites bearing mice into RPMI 1640 medium containing streptomycin and penicillin and were incubated in vitro for 48 h. The labeled compound was then added. After 1 h, the medium was centrifuged to separate the cells. Cells were counted to determine their activity uptake. DNA was extracted by addition of perchloric acid, followed by incubation for 1 h and centrifugation at 5000 rpm. The precipitate was counted in a γ-ray counter. The experiment was repeated with different incubation times (2, 4, 6, 16, and 32 h), and the DNA activity was counted at each time. Also the activity of cell constituents was counted, and the ratio was calculated between the DNA-incorporated activity and the activity in other constituents of the cell [13].

RESULTS AND DISCUSSION

Electrophoresis. The figure illustrates the activity distribution in electrophoresis. Two main peaks were formed, one corresponding to the free iodide that moved toward the anode with 16 cm distance. The second peak (^{125}I-Q_3D) stayed near the point of spotting and was similar to that of ^{125}I-iododeoxyuridine under the same electrophoretic conditions [14].

Factors affecting labeling yield. *Effect of oxidant amount.* We found that the electrophilic substitution of the iodonium ion [I^+] in the Q_3D molecule occurred with a high radiochemical yield when using CAT as an

Table 1. Effect of CAT content on the radiochemical yield of ^{125}I-Q_3D[a]

CAT amount, μg	Labeled compound yield, %	Free I^- content, %
10	87.2 ± 0.4	12.8 ± 0.3
25	88.6 ± 0.5[b]	12.4 ± 0.8
50	96.6 ± 0.5[b,c]	3.4 ± 0.1
100		3.8 ± 0.4

[a] Mean ± SEM, n = 6; the same in Tables 3–7.

[b] Significantly different from the initial values using unpaired Student's t-test ($p < 0.05$).

[c] Significantly different from the previous values using unpaired Student's t-test ($p < 0.05$).

Table 2. Effect of Q_3D content on the labeling yield

Q_3D amount, μg	Labeled compound yield, %	Free I^- content, %
10	88.4 ± 0.3	11.6 ± 0.4
25	94.5 ± 0.4[a,b]	5.5 ± 0.3
50	94.1 ± 0.4[a]	5.9 ± 0.3
100	95.2 ± 0.3[a]	4.8 ± 0.4
200	94.5 ± 0.3[a]	5.5 ± 0.3

[a] Significantly different from the initial values using unpaired Student's t-test ($p < 0.05$); the same in Tables 3–5.

[b] Significantly different from the previous values using unpaired Student's t-test ($p < 0.05$); the same in Tables 3–5.

Table 3. Effect of pH of the reaction medium on the ^{125}I-Q_3D yield

pH	Labeled compound yield, %	Free I^- content, %
2	68.4 ± 0.1	31.6 ± 0.2
4	90.2 ± 0.4[a]	9.8 ± 0.6
7	97.3 ± 0.3[a,b]	2.8 ± 0.2
9	93.2 ± 0.4[a,b]	6.8 ± 0.5
11	81.7 ± 0.2[a,b]	18.3 ± 0.4

Table 4. Effect of reaction time on the ^{125}I-Q_3D yield

Time, min	Labeled compound yield, %	Free I^- content, %
1	83.5 ± 0.4	16.5 ± 0.6
5	90.6 ± 0.3[a]	9.4 ± 0.9
10	91.3 ± 0.2[a]	8.7 ± 0.7
15	96.5 ± 0.4[a,b]	3.5 ± 0.2
30	96.6 ± 0.5[a,b]	3.4 ± 0.4[a,b]
60	97.1 ± 0.1[a,b]	2.9 ± 0.3

oxidizing agent (Table 1). The radiochemical yield significantly increased with an increase in the CAT amount from 10 to 50 μg (optimum content at which the maximum labeling yield was obtained). At the CAT amount increased over 50 μg, the yield showed no significant change. Apparently, at CAT amounts below 50 μg the CAT concentration is insufficient to convert all the iodide to iodonium ions, and the yield decreases [15].

Effect of substrate content on the labeling yield using CAT as an oxidizing agent is shown in Table 2. With an increase in the concentration of the starting material, the total incorporation of radioiodine usually increases, because there is a minimum limit to the volume used [16]. In our case, the yield appreciably increased with an increase in the Q_3D amount up to 25 μg, whereas larger amounts did not significantly affect the labeling yield.

Effect of pH. As shown in Table 3, pH 7 is the optimum pH at which the maximum yield was obtained (97.3%). The difference between the yields obtained at all the pH values was significant.

Effect of reaction time. Table 4 shows the relationship between the reaction time and the yield of ^{125}I-Q_3D. The radiochemical yield significantly increased from 56.9 to 94.8% with an increase in the reaction time from 1 to 15 min, but at the reaction time extended to 60 min no significant changes were observed.

In vitro stability of ^{125}I-Q_3D. No significant changes in the relative content of ^{125}I-Q_3D were observed for up to 48 h post labeling (Table 5). That is, the labeled compound is very stable.

Biodistribution of ^{125}I-Q_3D. *Normal mice.* Experiments showed (Table 6) that ^{125}I-Q_3D was distributed rapidly in blood, stomach, heart, and kidneys (15 min post injection). After 1 h, the ^{125}I-Q_3D uptake significantly decreased in blood, heart, liver, and spleen but

Table 5. Effect of time on the stability of ^{125}I-Q_3D

Time, min	Labeled compound content, %	Free I^- content, %
1	96.3 ± 0.1	4.7 ± 0.1
4	95.4 ± 0.7	4.6 ± 0.2
12	95.4 ± 0.4	4.6 ± 0.2
24	95.1 ± 0.1	4.9 ± 0.2
48	95.3 ± 0.5[a,b]	4.7 ± 0.4

Table 6. Biodistribution of ^{125}I-Q$_3$D in normal mice (% I.D./g)[a]

Organ, tissue	Normal mice				Ascites bearing mice			
	15 min	1 h	4 h	24 h	15 min	1 h	4 h	24 h
Blood	16.0 ± 0.1	13.4 ± 0.2[a]	6.40 ± 0.04[a]	3.7 ± 0.3[a]	11.7 ± 1.1	9.8 ± 0.4[b]	7.1 ± 0.1[b]	3.2 ± 0.2[b]
Bones	1.60 ± 0.05	1.9 ± 0.1[a]	0.9 ± 0.1[a]	0.7 ± 0.1[a]	2.1 ± 0.2	2.5 ± 0.2[b]	2.4 ± 0.2	1.8 ± 0.2[b]
Muscles	1.30 ± 0.01	1.70 ± 0.02[a]	1.6 ± 0.1	0.50 ± 0.02[a]	2.20 ± 0.09	2.70 ± 0.02[b]	2.10 ± 0.01[b]	0.70 ± 0.04[b]
Liver	2.40 ± 0.05	1.8 ± 0.2[a]	1.10 ± 0.06[a]	1.00 ± 0.02	4.7 ± 0.3	3.2 ± 0.2[b]	2.80 ± 0.06[b]	1.50 ± 0.07[b]
Lungs	5.7 ± 0.1	8.0 ± 0.1[a]	3.0 ± 0.2[a]	1.00 ± 0.01[a]	6.5 ± 0.1	4.20 ± 0.04[b]	3.1 ± 0.1[b]	0.5 ± 0.1[b]
Heart	9.0 ± 0.8	6.4 ± 0.3[a]	4.00 ± 0.01[a]	1.70 ± 0.04[a]	7.3 ± 0.3	6.1 ± 0.4[b]	3.1 ± 0.1[b]	1.4 ± 0.1[b]
Stomach	12.2 ± 0.9	16.2 ± 0.6[a]	9.6 ± 0.2[a]	5.7 ± 0.2[a]	9.6 ± 0.3	13.4 ± 0.9[b]	10.7 ± 0.6[b]	6.0 ± 0.5[b]
Intestine	6.4 ± 0.5	5.2 ± 0.3[a]	3.5 ± 0.1[a]	1.50 ± 0.03[a]	7.6 ± 0.5	6.40 ± 0.07[b]	4.4 ± 0.1[b]	2.9 ± 0.2[b]
Kidneys	9.7 ± 0.4	8.2 ± 0.6[a]	3.1 ± 0.3[a]	1.50 ± 0.06[a]	6.1 ± 0.4	3.4 ± 0.1[b]	2.0 ± 0.1[b]	1.20 ± 0.06[b]
Spleen	2.4 ± 0.3	1.3 ± 0.1[a]	1.00 ± 0.02	0.80 ± 0.05[a]	2.2 ± 0.1	1.70 ± 0.01[b]	1.10 ± 0.01[b]	0.30 ± 0.01[b]
Thyroid	0.70 ± 0.02	1.0 ± 0.1[a]	4.1 ± 0.2[a]	5.2 ± 0.2	2.10 ± 0.02	4.40 ± 0.04[b]	7.40 ± 0.06[b]	8.20 ± 0.05
Ascitic fluid	–	–	–	–	3.5 ± 0.3	5.2 ± 0.4[b]	7.1 ± 0.1[b]	5.80 ± 0.05

[a] Significantly different from the previous values using unpaired Student's *t*-test ($p < 0.05$).

[b] Significantly different from the initial values using unpaired Student's *t*-test ($p < 0.05$).

significantly increased in stomach, bones, muscles, and thyroid. At 4 and 24 h post injection, the majority of tissues showed significant decrease in the ^{125}I-Q$_3$D uptake except the thyroid gland in which the uptake increased.

Ascites bearing mice. The sites of the highest uptake of ^{125}I-Q$_3$D at 15 min post injection were the blood, stomach, heart, and intestine (11.7, 12.3, 7.3, and 7% I.D./g, respectively). Table 6 shows that the concentration of ^{125}I-Q$_3$D at 15 min post injection was the lowest in thyroid, muscles, and spleen. The ^{125}I-Q$_3$D uptake in ascitic fluid was rapid (3.5% I.D./ml in the first 15 min). The uptake in ascitic fluid significantly increased in the first 4 h and then somewhat decreased. Increased uptake at 1 h post injection was also observed in stomach, kidneys, and thyroid gland, whereas in blood, heart, and lungs at the same time the uptake decreased. At 4 h post injection, the majority of organs showed significant decrease in the ^{125}I-Q$_3$D uptake. Significant increase was only observed in ascitic fluid and thyroid gland. Similarly, at 24 h post injection, the majority of organs showed additional significant decrease in the ^{125}I-Q$_3$D uptake. The experiments showed that ascites was one of the sites of the strongest ^{125}I-Q$_3$D uptake at both l and 24 h post injection. The overall ^{125}I-Q$_3$D uptake in ascites (fluid volume 3.2 ± 0.7 ml) was about 40% of the injected dose at 4 h post injection. This result indicates that ^{125}I-Q$_3$D shows promise for tumor imaging. The high uptake of ^{125}I-Q$_3$D in kidneys may reflect the excretion of the drug via urine [3]. The observation that the ^{125}I-Q$_3$D concentration in the thyroid was significantly lower than in other tissues indicates that the amount of the free iodide was low, as free iodide is rapidly captured by thyroid [17]. However, thyroid uptake increased with time from 4.4% at 1 h to 7.4% at 4 h post injection due to in vivo deiodination of ^{125}I-Q$_3$D [16, 18].

DNA extraction. The increase in the incubation time was associated with significant increase in the associated activity percentage. More than 60% of the total activity was associated with DNA (Table 7). This means that the DNA-associated activity was transferred from cells to daughter cells in chromosomes.

Table 7. Comparison between DNA-incorporated activity and activity in other constituent of the cell

Incubation time, h	Activity associated with DNA, %	Activity in other constituents of cells, %
1	12 ± 0.7	88 ± 0.7
2	18 ± 2[a]	82 ± 2[a,b]
4	24 ± 2[a]	76 ± 2[a,b]
8	35 ± 1[a]	65 ± 1[a,b]
16	45.0 ± 0.8[a]	55.0 ± 0.8[a,b]
32	62.0 ± 0.9[a]	38.0 ± 0.9[a,b]

[a] Significantly different from the initial values using unpaired Student's *t*-test ($p < 0.05$); $n = 10$.

[b] Significantly different from the previous values using unpaired Student's *t*-test ($p < 0.05$).

Thus, the incorporation of an Auger emitter (^{125}I) into a tumor site was achieved by labeling of Q_3D with ^{125}I. The appropriate conditions for labeling of ^{125}I-Q_3D (95% yield) are as follows: 50 μg of CAT as oxidizing agent, 25 μg of Q_3D as substrate, pH 7, room temperature, 15 min. High incorporation of ^{125}I-Q_3D in tumor sites (ascites tumor) facilitates tumor imaging. ^{125}I-Q_3D is convenient to transport ^{125}I to the nucleus of tumor cells. It seems appropriate to further study this radiolabeled compound in vivo and in vitro using different cancer cell lines.

REFERENCES

1. Wally, M.A., El-Gogray, S.R., and El-Sepelgy, O.Z., *Synth. Commun*., 2010, vol. 40, pp. 1–5.
2. Adelstein, S.J. and Kassis, A.I., *Acta Oncol*., 1996, vol. 35, no. 7, p. 797.
3. Kassis, A.I., Kirichian, A.M., Wang, K., et al., *Int. J. Radiat. Biol*., 2004, vol. 80, p. 941.
4. Kassis, A.I., *J. Nucl. Med.*, 2003, vol. 44, p. 1479.
5. Ibrahim, I.T. and Wally, M.A., *J. Radioanal. Nucl. Chem*., 2010, vol. 285, pp. 169–175.
6. Pressacco, J., Hedley, D.W., and Erlichman, C., *Cancer Res*., 1994, vol. 54, p. 3772.
7. Mester, J., DeGoeij, K., and Sluyser, M., *Eur. J. Cancer*, 1996, vol. 32, p. 1603.
8. Issidorides, C.H. and Haddadin, M.J., *J. Org. Chem*., 1966, vol. 31, p. 4067.
9. Korde, A., Venkatesh, M., and Sarma, H.D., in *Int. Symp. on Modern Trends in Radiopharmaceuticals for Diagnosis and Therapy*, Lisbon (Portugal), March 30–April 3, 1998, IAEA, SM-355/13.
10. Walicka, M.A., Adelstein, S.J., and Kassis, A.I., *Radiat. Res*., 1998, vol. 149, p. 134.
11. Bodei, L., Kassis, A.I., Adelstein, S.J., and Mariani, G., *Cancer Biother. Radiopharm*., 2003, vol. 18, no. 6, p. 861.
12. Chen, K., Adelstein, S.J., and Kassis, A.I., *Int. J. Radiat. Biol*., 2004, vol. 80, nos. 11–12, p. 921.
13. Greene, R.F. and Collins, J.M., *Cancer Res*., 1990, vol. 50, p. 6652.
14. Coenen, H.H. and Wilbur, D.S., *Bioconjugate Chem*., 1992, vol. 3, p. 433.
15. Darnowski, J.W. and Goulette, F.A., *Biochem. Pharmacol*., 1994, vol. 48, p. 1797.
16. Noaman, E., Salem, H.A., Motaleb, M.A., et al., *Arab J. Nucl. Sci. Appl*., 2007, vol. 37, p. 1.
17. Nair, S.C., Pannikar, B., and Panikkar, K.R., *Cancer Lett*., 1991, vol. 57, no. 2, p. 109.
18. Desombre, E.R., *Cancer Res*., 1992, vol. 52, p. 5752.